Werk

Jahr: 1979
Kollektion: fid.geo
Signatur: 8 Z NAT 2148:46
Digitalisiert: Niedersächsische Staats- und Universitätsbibliothek Göttingen
Werk Id: PPN1015067948_0046
PURL: http://resolver.sub.uni-goettingen.de/purl?PPN1015067948_0046

LOG Id: LOG_0036
LOG Titel: Approximate diffraction theory for transparent half-planes with application to seismic-wave diffraction at coal seams
LOG Typ: article

Übergeordnetes Werk

Werk Id: PPN1015067948
PURL: http://resolver.sub.uni-goettingen.de/purl?PPN1015067948
OPAC: http://opac.sub.uni-goettingen.de/DB=1/PPN?PPN=1015067948

Contact

Niedersächsische Staats- und Universitätsbibliothek Göttingen
Georg-August-Universität Göttingen
Platz der Göttinger Sieben 1
37073 Göttingen
Germany
Email: gdz@sub.uni-goettingen.de

J. Geophys. 46, 349–367, 1979

Journal of Geophysics

Approximate Diffraction Theory for Transparent Half-Planes With Application to Seismic-Wave Diffraction at Coal Seams

J. Fertig* and G. Müller**

Geophysical Institute, University of Karlsruhe, Hertzstr. 16, D-7500 Karlsruhe, Federal Republic of Germany

Abstract. Starting with the exact theory of diffraction of plane SH or plane acoustic P waves at an opaque half-plane, i.e., a rigid screen or a crack, an approximate theory is given for diffraction at a transparent half-plane, realized, e.g., by a thin layer in a homogeneous medium. The results are extended for linesource excitation. The diffraction formula is similar to formulas based on Kirchhoff diffraction theory, but it includes both a term related to the reflected wavefield and a term related to the direct plus transmitted field. Moreover, use is made of the reciprocity principle. A comparison with finite-difference calculations for SH waves shows that the approximate theory has a rather broad range of applicability. Results of calculations are presented which are related to wave-propagation problems encountered in seismic prospecting for coal: the reflections and diffractions generated by a sequence of coal seams with an offset along a fault are calculated, and the diffractions produced by a realistic vertical offset of a horizontal seam are studied in some detail.

Key words: Diffraction theory – Theoretical seismograms – Seismic prospecting for coal.

Introduction

The seismic reflection response of coal-seam sequences normally has a complicated pattern. The three main reasons for this are: (1) the seams are often closely grouped such that individual seams cannot be resolved even with high frequencies, (2) wave conversion upon oblique incidence of the wave from the source can produce strong additional reflections, (3) seam offsets due to faults

* *Present address:* Preussag AG, Erdöl und Erdgas, Arndtstr. 1, D-3000 Hannover, Federal Republic of Germany

** *Present address:* Institute of Meteorology and Geophysics, University of Frankfurt, Feldbergstr. 47, D-6000 Frankfurt, Federal Republic of Germany

0340-062X/79/0046/0349/$03.80

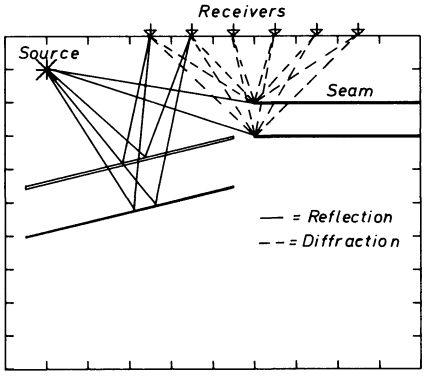

Fig. 1. Two-dimensional model with an arbitrary number of seams of finite width, and reflected and diffracted rays from the line source to the receivers

cause diffractions and offsets in the reflections. We have investigated the first two effects in an earlier paper (Fertig and Müller, 1978) with the aid of the reflectivity method and assumed for these purposes horizontally layered seam sequences without offsets. In the present paper we are mainly interested in the effects produced by the interruption and termination of seams due to faulting, and we present an approximate method for the calculation of theoretical seismograms in such cases. Such theoretical seismograms can help to clarify the circumstances under which coal-seam offsets can be detected by seismic measurements.

Our model of the subsurface is two-dimensional, the source of waves is a line source, and we consider only the SH-wave and the acoustic P-wave case. This is a restriction to the simplest conditions of wave propagation which, nevertheless, are of practical importance; for instance, SH-waves may well become a more routinely used tool in seismic exploration because of their greater simplicity and resolving power, compared with P-waves. The seams are assumed to be thin plane layers of finite width, located horizontally or non-horizontally in an otherwise homogeneous medium (Fig. 1). The plane-wave reflection and transmission response of an individual seam is calculated with the reflectivity method and corrected by the geometrical-spreading factor of cylindrical waves. Multiples between the seams are disregarded; calculations for horizontal seam sequences with the reflectivity method, which yield also these multiples, show that this neglection is often permitted, inspite of the large reflection coefficients of coal seams. The diffractions from the seam ends are calculated with an approximate theory which is an extension of the exact theory of diffraction of plane SH-waves at an opaque half-plane. This approximate diffraction theory is described in the first part of the paper, and its results for a special case are compared with the results of finite-difference calculations.

Later in this paper we present a few examples of theoretical seismogram sections. The computations illustrate the reflection and diffraction of P waves at a single seam, and at a sequence of dipping seams which are separated into two blocks by a fault. Finally, we investigate the reflection, transmission and diffraction of P and SH waves at a realistic vertical offset of a horizontal seam.

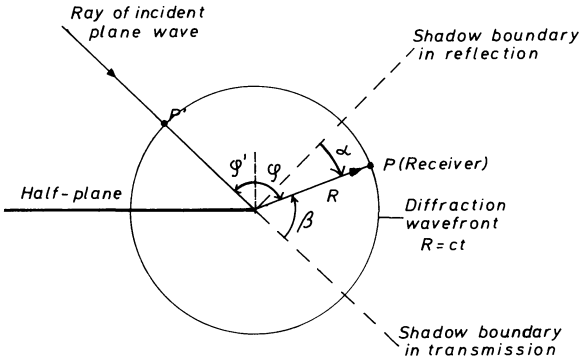

Fig. 2. Definition of diffraction angles α and β, relative to the shadow boundaries, and of the angles φ' and φ. α and β as indicated are positive

Approximate Diffraction Theory for a Transparent Half-Plane

Plane-Wave Excitation. Our starting point is the exact theory of diffraction of a plane SH wave with unit-step function time behavior at an opaque half-plane (either a rigid screen or a crack), as given, e.g., by Pao and Mow (1973, pp. 572–586). In a first step, we introduce into their formulas (5.15) for a rigid screen and (5.22) for a crack the diffraction angles α and β with respect to the shadow boundaries in reflection and transmission (see Fig. 2). Then, we observe that Pao and Mow's formulas give the *total* displacement field for distances R from the edge of the half-plane less than or equal to ct, where c is the S-wave velocity of the medium and t the time relative to the arrival of the incident plane wave at the edge. In order to obtain the *diffracted* displacement field alone we have to subtract the direct wave for receivers with $\alpha>0$ and $\beta>0$, and the direct plus the reflected wave for receivers with $\alpha<0$ and $\beta>0$. The result is:

$$\Psi^{(0)}_{\text{diff}}=\frac{1}{\pi}\left\{r\arctan\frac{\left[\frac{c}{2R}\left(t-\frac{R}{c}\right)\right]^{\frac{1}{2}}}{\sin\frac{\alpha}{2}}-\arctan\frac{\left[\frac{c}{2R}\left(t-\frac{R}{c}\right)\right]^{\frac{1}{2}}}{\sin\frac{\beta}{2}}\right\}H\left(t-\frac{R}{c}\right) \tag{1}$$

The coefficient r is -1 for a rigid screen and $+1$ for a crack, and $H(t)$ is the unit-step function.

The first term in (1) dominates close to the shadow boundary in reflection, where it is discontinuous and jumps from $rH(t-R/c)/2$ for $\alpha>0$ to $-rH(t-R/c)/2$ for $\alpha<0$. If for $\alpha<0$ the reflection $rH(t-R/c)$ is superposed, the total wave field is continuous at the shadow boundary in reflection, as it should be. Similarly, the second term in (1) dominates close to the shadow boundary in transmission ($\beta=0$). Its discontinuity is removed by adding, for $\beta>0$, the direct wave.

The generalization of the first term of (1) for a transparent half-plane is straightforward, if one considers the fact that r in (1) is just the plane-wave reflection coefficient of the half-plane. As in usual Kirchhoff diffraction theory,

one obtains a convolution of the plane-wave reflection response $r(t)$ of the half-plane [or more precisely of its derivative $r'(t)$] with a diffraction operator which here is the first arc tan function in (1). The second term in (1) has to be interpreted as the contribution to diffraction from the direct wave. In order to generalize this term for a transparent half-plane we have to include additionally a contribution from the transmitted wave on the underside of the half-plane. If the direct wave is $d(t)$ [not necessarily equal to $H(t)$] and the plane-wave transmission response of the half-plane $b(t)$, we arrive at the convolution of the difference $b'(t)-d'(t)$ and the second arc tan function in (1). The total diffraction is

$$\Psi_{\text{diff}}^{(1)} = r'(t) * \frac{1}{\pi} H\left(t-\frac{R}{c}\right) \arctan \frac{\left[\frac{c}{2R}\left(t-\frac{R}{c}\right)\right]^{\frac{1}{2}}}{\sin\frac{\alpha}{2}}$$

$$+ [b'(t)-d'(t)] * \frac{1}{\pi} H\left(t-\frac{R}{c}\right) \arctan \frac{\left[\frac{c}{2R}\left(t-\frac{R}{c}\right)\right]^{\frac{1}{2}}}{\sin\frac{\beta}{2}}.$$

This formula has the disadvantage that it does not satisfy the reciprocity principle which in the present case requires unchanged displacements, when (Fig. 2) the receiver is shifted to P' and the ray of the incident plane wave passes through P. In an ad-hoc procedure we enforce reciprocity by averaging the two diffractions; this step, of course, needs justification which will be given later. Averaging the diffractions is equivalent to averaging the plane-wave reflection and transmission responses, since the diffraction operators are the same. If we define

$\bar{r}(t)[\bar{b}(t)]$ = arithmetic mean of the half-plane reflection (transmission) responses to a plane wave $d(t)$ with angle of incidence φ' and φ, respectively (see Fig. 2),

we obtain the final diffraction formula for plane-wave excitation:

$$\Psi_{\text{diff}}^{(2)} = \bar{r}'(t) * \frac{1}{\pi} H\left(t-\frac{R}{c}\right) \arctan \frac{\left[\frac{c}{2R}\left(t-\frac{R}{c}\right)\right]^{\frac{1}{2}}}{\sin\frac{\alpha}{2}}$$

$$+ [\bar{b}'(t)-d'(t)] * \frac{1}{\pi} H\left(t-\frac{R}{c}\right) \arctan \frac{\left[\frac{c}{2R}\left(t-\frac{R}{c}\right)\right]^{\frac{1}{2}}}{\sin\frac{\beta}{2}} \tag{2}$$

Discussion of Formula (2). For an opaque half-plane and the direct wave $d(t) = H(t)$, we have $\bar{r}(t) = \pm H(t)$ and $\bar{b}(t) = 0$, and (2) reduces to (1). Moreover, $\Psi_{\text{diff}}^{(2)}$ satisfies all continuity requirements of the total field at the wavefront of the

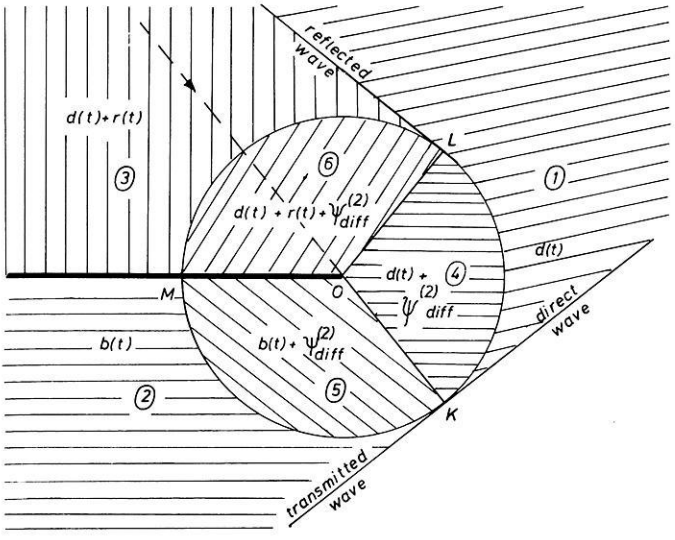

Fig. 3. Wave fronts for reflection, transmission and diffraction of a plane SH wave at a transparent half-plane. The total displacement in six different domains is indicated. For details see text

diffraction and at the shadow boundaries. In order to show this, we consider the wavefront picture for a fixed time in Fig. 3; it is subdivided into six different domains in each of which the *total* displacement field is indicated. The displacements at the wavefront of the diffraction are continuous, since $\Psi^{(2)}_{\text{diff}}$ starts from zero at $t=R/c$. The continuity of the displacements at the shadow boundaries OK and OL will now be demonstrated in the case of OK. The first term of (2) is continuous across OK. The second term in domain ⑤ close to OK (i.e., for small negative β) is

$$[\bar{b}'(t)-d'(t)]*\frac{1}{\pi}H\left(t-\frac{R}{c}\right)\frac{-\pi}{2}\approx-\tfrac{1}{2}b\left(t-\frac{R}{c}\right)+\tfrac{1}{2}d\left(t-\frac{R}{c}\right),$$

and in domain ④, also close to OK, it is

$$[\bar{b}'(t)-d'(t)]*\frac{1}{\pi}H\left(t-\frac{R}{c}\right)\frac{\pi}{2}\approx\tfrac{1}{2}b\left(t-\frac{R}{c}\right)-\tfrac{1}{2}d\left(t-\frac{R}{c}\right).$$

The total field in ⑤ close to OK is (addition of the transmitted wave)

$$\tfrac{1}{2}b\left(t-\frac{R}{c}\right)+\tfrac{1}{2}d\left(t-\frac{R}{c}\right)+\text{first term of (2)},$$

and in ④, also close to OK, it is (addition of the direct wave)

$$\tfrac{1}{2}b\left(t-\frac{R}{c}\right)+\tfrac{1}{2}d\left(t-\frac{R}{c}\right)+\text{first term of (2)},$$

i.e., the total field is continuous across OK. Similar results hold for the shadow boundary OL.

A limitation of the simple diffraction formula (2) is that $\Psi_{\text{diff}}^{(2)}$ for transparent half-planes does not satisfy the boundary conditions at points on the half-plane between O and M (Fig. 3). There is no direct way to determine the degree of disagreement, since in the framework of the simple theory presented only the plane-wave reflection and transmission responses of the half-plane are needed; the field inside the half-plane does not enter. All that can be done is to test (2) against exact results, calculated, e.g., with finite-difference methods. This will be discussed later.

In geophysical applications of (2) the transparent half-plane will be a homogeneous layer (e.g., a coal seam) or even a layer with internal layering. It is clear that (2) can only be used, if the dominant wavelength is at least several times the layer thickness. Furthermore, the S velocity *in* the layer should be less than in the surrounding medium, since otherwise refraction along the layer would occur and diffraction at the edge would start before the direct wave arrives there. Probably this contribution is small, but a more detailed investigation is necessary before one can conclude that (2) is a useful approximation also in the case of a high-velocity layer.

Line-Source Excitation. In a final step we derive from (2) the diffracted field due to excitation by a line source whose distance from the diffracting edge is R'. The incident wave at the edge is assumed to be

$$\Psi_{\text{inc}} = \frac{1}{R'^{\frac{1}{2}}} d\left(t - \frac{R'}{c}\right), \tag{3}$$

i.e., the line source radiates isotropically, beginning at $t=0$, and geometrical spreading is that for cylindrical waves. The corresponding formula for Ψ_{diff} should satisfy the following plausible requirements [see (2) for reference]:

(a) The first term should be, for sufficiently small α,

$$\frac{\operatorname{sign}\alpha}{2(R'+R)^{\frac{1}{2}}} r(t-t_d),$$

i.e., half the reflection response at the shadow boundary (apart from the sign). Likewise for small β the second term should be

$$\frac{\operatorname{sign}\beta}{2(R'+R)^{\frac{1}{2}}} [b(t-t_d) - d(t-t_d)].$$

Here and in the following, $t_d = (R'+R)/c$ is the arrival time of the diffraction.

(b) For larger values of α the first term of Ψ_{diff} should be $1/R'^{\frac{1}{2}}$ times the first term of (2), i.e.,

$$\frac{\bar{r}'(t)}{R'^{\frac{1}{2}}} * \frac{1}{\pi} H(t-t_d) \arctan \frac{\left[\frac{c}{2R}(t-t_d)\right]^{\frac{1}{2}}}{\sin\frac{\alpha}{2}}, \tag{4}$$

and similarly the second term of Ψ_{diff} for larger β should be

$$\frac{\bar{b}'(t)-d'(t)}{R'^{\frac{1}{2}}} * \frac{1}{\pi} H(t-t_d) \arctan \frac{\left[\frac{c}{2R}(t-t_d)\right]^{\frac{1}{2}}}{\sin\frac{\beta}{2}}. \tag{5}$$

The following form of Ψ_{diff} satisfies these requirements:

$$\Psi_{\text{diff}} = \frac{\bar{r}'(t)}{(R'+R)^{\frac{1}{2}}} * \frac{1}{\pi} H(t-t_d) \arctan \frac{\left[\frac{c}{2R}(t-t_d)\right]^{\frac{1}{2}}}{\left(\frac{R'}{R'+R}\right)^{\frac{1}{2}} \sin\frac{\alpha}{2}}$$

$$+ \frac{\bar{b}'(t)-d'(t)}{(R'+R)^{\frac{1}{2}}} * \frac{1}{\pi} H(t-t_d) \arctan \frac{\left[\frac{c}{2R}(t-t_d)\right]^{\frac{1}{2}}}{\left(\frac{R'}{R'+R}\right)^{1/2} \sin\frac{\beta}{2}} \tag{6}$$

The first of the above conditions is fulfilled, since for small α or β the additional term in the argument of the arc tan functions, $[R'/(R'+R)]^{\frac{1}{2}}$, does not change the step-function behavior of the diffraction operators. The second condition is approximately satisfied, since for larger α and β the arc tan functions in (4), (5) and (6) can be expanded into Taylor series with restriction to the first term. In this approximation, which actually is a high-frequency or wavefront approximation, (4) and the first term of (6) agree, and likewise (5) and the second term.

Formula (6) was derived for SH waves, and Ψ_{diff} is the out-of-plane displacement of the diffracted wave. This formula can also be used for acoustic P waves. In this case Ψ_{inc} in (3) or Ψ_{diff} in (6) can be either the displacement potential, the pressure or the displacement along the ray, and $\bar{r}(t)$ and $\bar{b}(t)$ are the averaged compressional reflection and transmission responses. In the applications, given later in this paper, mainly the acoustic case is treated. Formula (6) can, in principle, also be applied in the case of P-SV waves in solid media; a few corresponding remarks are made at the end of this paper.

The treatment of diffraction at a half-plane with Kirchhoff diffraction theory (Berryhill, 1977; Trorey, 1977) so far has given results similar to the first term in (6). No contribution similar to the second term has been found. The reason is that only backward diffraction was of interest and hence only the reflected field at the topside of the half-plane was continued upwards by Kirchhoff's formula. However, depending on the parameter contrasts between the half-plane and the surrounding medium and hence on the difference between the direct wave $d(t)$ and the averaged transmission response $\bar{b}(t)$, the second term in (6) which dominates the forward diffraction can also be of importance for backward diffraction. Another difference to Kirchhoff diffraction theory is the incorporation of reciprocity in (6) which gives a considerably broader range of applicability, as will be seen later.

Comparison of the Approximate Diffraction Theory With Finite-Difference Calculations

To test formula (6) we computed synthetic seismograms, both with (6) and with a finite-difference method, for vertical incidence of an SH wave on a transparent half-plane which is represented by a thin homogeneous layer.

Plane-Wave Response of a Homogeneous Layer. In the following we summarize the formulas which describe the reflection and transmission of a plane wave $d(t)$ by a homogeneous layer of infinite extent in all directions, embedded in a full-space. Besides the SH-wave case we consider also the acoustic P-wave case. The full-space is characterized by the P velocity α_1, the S velocity β_1 and the density ρ_1. The corresponding parameters of the layer are α_2, β_2 and ρ_2; its thickness is h. The plane-wave reflection and transmission coefficients, r_{ss} or r_{pp} and b_{ss} or b_{pp}, for monochromatic waves of circular frequency ω are (j = imaginary unit):

SH waves	Acoustic P waves	
$r_{ss}=\dfrac{r_0(1-E)}{1-r_0^2E}$	$r_{pp}=\dfrac{r_0(1-E)}{1-r_0^2E}$	(7)
$b_{ss}=\dfrac{1-r_0^2}{1-r_0^2E}$	$b_{pp}=\dfrac{1-r_0^2}{1-r_0^2E}$	(8)

$$E=\exp\left(-2j\omega\frac{h}{v}\cos\varphi_2\right)$$

$v=\beta_2$	$v=\alpha_2$	
$r_0=\dfrac{\rho_1\beta_1\cos\varphi_1-\rho_2\beta_2\cos\varphi_2}{\rho_1\beta_1\cos\varphi_1+\rho_2\beta_2\cos\varphi_2}$	$r_0=\dfrac{\rho_2\alpha_2\cos\varphi_1-\rho_1\alpha_1\cos\varphi_2}{\rho_2\alpha_2\cos\varphi_1+\rho_1\alpha_1\cos\varphi_2}$	(9)

φ_1 is the angle of incidence, and φ_2 the angle of refraction in the layer, related to φ_1 by Snell's law. r_0 is the plane-wave reflection coefficient of the upper boundary of the layer.

The reflection and transmission responses of the layer, $r(t)$ and $b(t)$, which are needed in the diffraction formula (6), follow from (7) and (8) by multiplication with the spectrum of the incident wave $d(t)$ and by an inverse Fourier transform; both the angle φ' and φ, defined in Fig. 2, enters as the angle of incidence.

For wavelengths much longer than the layer thickness h the following low-frequency approximations are useful [they are obtained from (7) and (8) by power-series expansions in ω]:

$$\left.\begin{aligned} r(t)&=\frac{r_0\tau}{1-r_0^2}\,d'(t)\\ b(t)-d(t)&=-\frac{r_0^2\tau}{1-r_0^2}\,d'(t)=-r_0r(t)\\ \tau&=\frac{2h}{v}\cos\varphi_2. \end{aligned}\right\} \tag{10}$$

The error of these approximations is less than 10%, if the wavelength in the layer is greater than 15 to 20 times h.

With these results the diffraction for line-source excitation is readily obtained from (6). To obtain the complete wavefield we have to add the direct, reflected or transmitted wave, depending on where the receiver is located. These contributions are $L^{-\frac{1}{2}}$ times $d(t-L/c)$, $r(t-L/c)$ or $b(t-L/c)$, where L is the length of the wavepath from the line source to the receiver and c is either α_1 or β_1. $r(t)$ and $b(t)$ are determined for the corresponding angle of incidence which normally is different from the angles φ' and φ.

Finite-Difference Method. When finite-difference methods are applied to the wave propagation in heterogeneous media, one has the choice to use either the equation of motion for homogeneous media, combined with a formulation of the boundary conditions at the boundaries between different homogeneous parts of the medium, or to use the equation of motion for heterogeneous media. We chose the second method (Kelly et al., 1976), mainly because it allows also the modelling of complicated structures. The two-dimensional equation of motion for SH waves in this case and for spatially constant density is

$$\frac{\partial^2 v}{\partial t^2}=\frac{\partial}{\partial x}\left(\beta^2\frac{\partial v}{\partial x}\right)+\frac{\partial}{\partial z}\left(\beta^2\frac{\partial v}{\partial z}\right). \tag{11}$$

Here, x and z are the two spatial coordinates, $v(x,z,t)$ is the out-of-plane displacement, and $\beta(x,z)$ the S velocity. The density was kept constant in order to save computer storage and time; including an inhomogeneous density distribution into (11) would pose no problems.

In the finite-difference approximation of (11) we use standard central differences. If the time step is Δt and the grid spacings are Δx and Δz, and if $v^M_{K,L}$ and $\beta_{K,L}$ are the discrete approximations of $v(K\Delta x, L\Delta z, M\Delta t)$ and $\beta(K\Delta x, L\Delta z)$, we obtain:

$$\frac{\partial^2 v}{\partial t^2}=\frac{1}{\Delta t^2}(v^{M+1}_{K,L}-2v^M_{K,L}+v^{M-1}_{K,L})$$

$$\begin{aligned}\frac{\partial}{\partial x}\left(\beta^2\frac{\partial v}{\partial x}\right)=\frac{1}{2\Delta x^2}&[(\beta^2_{K+1,L}+\beta^2_{K,L})(v^M_{K+1,L}-v^M_{K,L})\\&-(\beta^2_{K,L}+\beta^2_{K-1,L})(v^M_{K,L}-v^M_{K-1,L})]\end{aligned}$$

$$\begin{aligned}\frac{\partial}{\partial z}\left(\beta^2\frac{\partial v}{\partial z}\right)=\frac{1}{2\Delta z^2}&[(\beta^2_{K,L+1}+\beta^2_{K,L})(v^M_{K,L+1}-v^M_{K,L})\\&-(\beta^2{}_{K,L}+\beta^2_{K,L-1})(v^M_{K,L}-v^M_{K,L-1})]\end{aligned}$$

Then (11) yields for $\Delta z=\Delta x$:

$$\begin{aligned}v^{M+1}_{K,L}=&2v^M_{K,L}-v^{M-1}_{K,L}\\&+\left(\frac{\Delta t}{\Delta x}\right)^2[\beta^2_E(v^M_{K+1,L}-v^M_{K,L})-\beta^2_W(v^M_{K,L}-v^M_{K-1,L})\\&+\beta^2_S(v^M_{K,L+1}-v^M_{K,L})-\beta^2_N(v^M_{K,L}-v^M_{K,L-1})]\end{aligned} \tag{12}$$

$$\beta^2_E=\tfrac{1}{2}(\beta^2_{K+1,L}+\beta^2_{K,L})\qquad \beta^2_W=\tfrac{1}{2}(\beta^2_{K,L}+\beta^2_{K-1,L})$$

$$\beta^2_S=\tfrac{1}{2}(\beta^2_{K,L+1}+\beta^2_{K,L})\qquad \beta^2_N=\tfrac{1}{2}(\beta^2_{K,L}+\beta^2_{K,L-1})$$

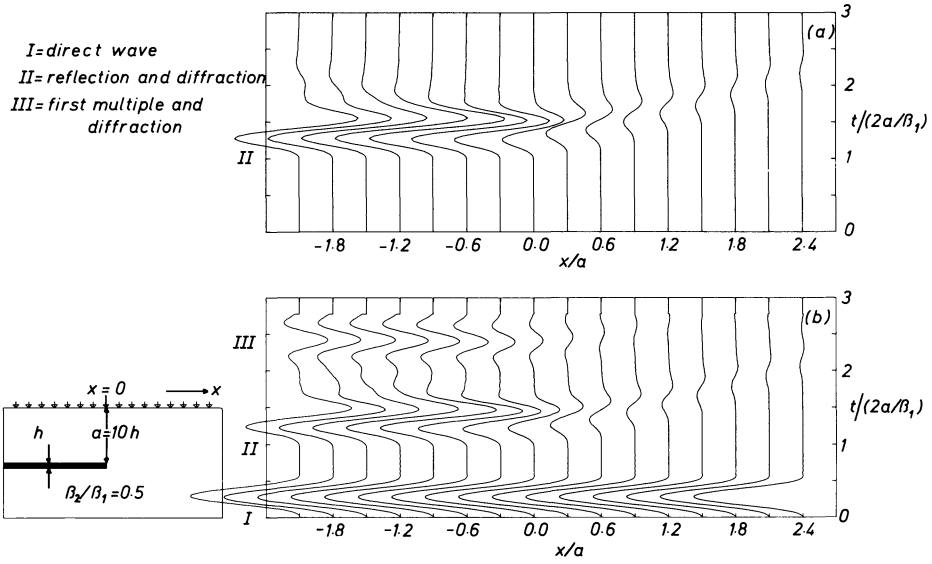

Fig. 4a and b. Reflection and diffraction of plane, vertically travelling SH waves at a transparent half-plane: **a** analytical calculation; **b** finite-difference calculation

To keep the explicit scheme (12) stable we use the relation $\Delta t = \Delta x/(\beta_{\max}\sqrt{2})$ between the time step and the grid spacing, where $\beta_{\max}$ is the maximum S velocity of the model (Boore, 1972). Grid dispersion is reduced by choosing Δx equal to about 1/12 of the dominant wavelength in those parts of the model with the minimum S velocity, $\beta_{\min}$.

The scheme (12) is supplemented by prescribed displacements at the source, by the boundary condition of vanishing stress at the boundaries of the rectangular model, and by initial conditions corresponding to vanishing displacements and particle velocities for $t=0$.

First-order discontinuities parallel to the x or z axis are modelled by a jump in β over one grid spacing and are thus located approximately in the middle between two neighbouring grid lines. In our numerical study of the reflection and diffraction of SH waves at a thin layer the layer velocity is assigned to two grid lines. Hence, if we want to calculate the response of a layer of thickness h, Δx is approximately $h/2$, and this value is used in our calculations. This is an approximation which can be wrong perhaps by 10 to 20%; only within these limits the finite-difference seismograms can be considered as exact and thus as a reference for analytically calculated seismograms.

Results. The model and the receiver geometry are illustrated in Fig. 4. A vertically travelling plane SH wave leaves the receiver level at $t=0$ and is reflected and diffracted at a thin layer with thickness h, velocity $\beta_2 = 0.5\,\beta_1$ and density $\rho_2 = \rho_1$. For the analytical calculation (Fig. 4a) formula (6) is used with a line source at large distance R' vertically above the diffracting edge, and corresponding time shifts and amplitude corrections are applied. The input

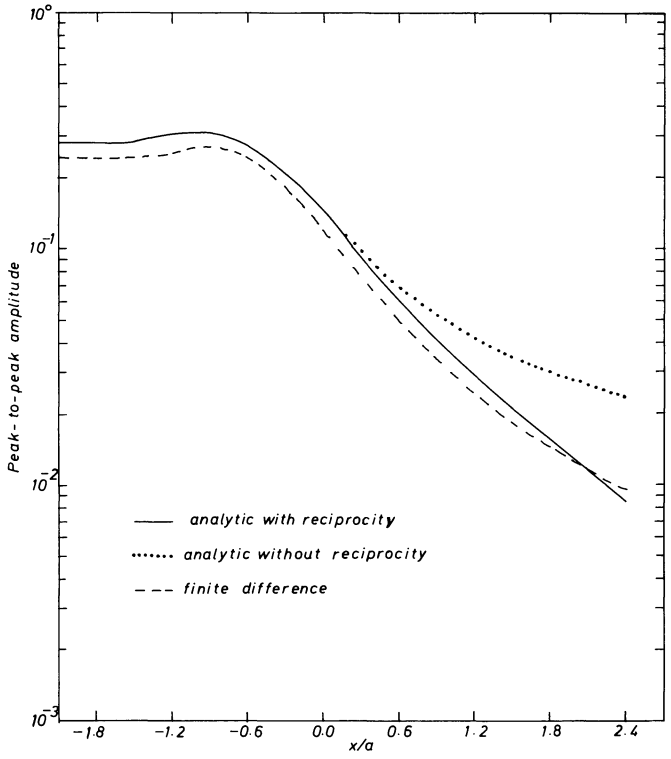

Fig. 5. Peak-to-peak amplitudes of the reflection and diffraction as a function of distance for the case shown in Fig. 4

signal has a simple bell-shaped form and unit maximum amplitude (see arrival I in Fig. 4b). The pulse duration corresponds to a length in the medium surrounding the layer of about 13 h and therefore is much larger than h. The distribution of receivers is symmetric with respect to the shadow boundary in reflection at $x = 0$. To the left of the shadow boundary one observes the reflection and the diffraction, to the right we have the diffraction alone. The finite-difference seismograms (Fig. 4b) display also the direct wave and the first multiple between the layer and the free surface, including the corresponding diffraction; the pulse forms of all three arrivals in Fig. 4b demonstrate nicely the differentiating effect of the reflection at thin layers. In the analytical calculation the receivers are assumed within the medium, whereas in the finite-difference calculation they are at the free surface which doubles the amplitudes of the reflections and diffractions. To correct for this difference the finite-difference seismograms were multiplied by 0.5. Hence, the reflections and diffractions in Fig. 4a and b are directly comparable.

The overall agreement of the pulse forms and amplitudes in this figure is quite good even to the largest distances x, i.e., to diffraction angles α up to 67°. A quantitative comparison of peak-to-peak amplitudes is given in Fig. 5. Taking into account the remarks made before on the accuracy of the finite-difference

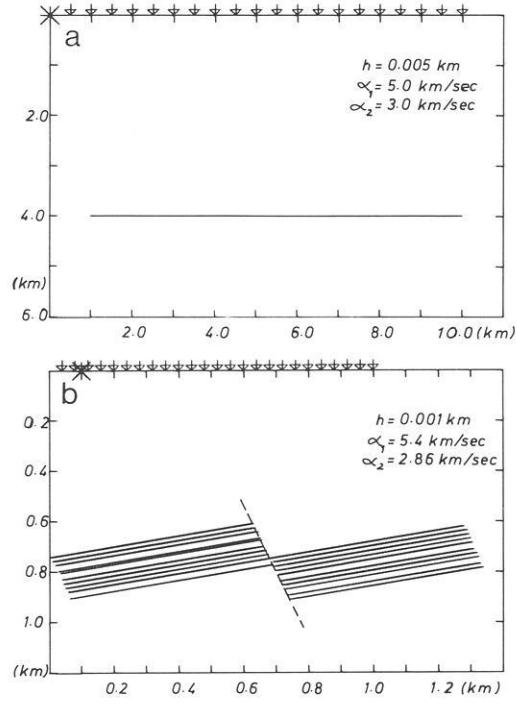

Fig. 6. a Thin layer of finite width embedded in a homogeneous medium. The positions of the line source and the receivers are marked at the top of the model. The density ratio is $\rho_2/\rho_1 = 0.85$.
b A sequence of coal seams which are offset by a fault. The density ratio is $\rho_2/\rho_1 = 0.82$

calculations, we conclude that the approximate diffraction formula (6) has a broad range of applicability and that the inclusion of reciprocity is a definite improvement. The limits of this formula are, however, reached when for fixed source position, i.e., for fixed angle of incidence φ' at the diffracting edge, and for variable receiver position, i.e., for variable angle φ, the averaged reflection response $\bar{r}(t)$ of the half-plane becomes zero or even changes its sign. [This cannot occur with the averaged transmission response $\bar{b}(t)$.] If the half-plane is a homogeneous layer whose P- and S-wave impedances are less than those of the surrounding medium, this can only happen in the case of SH waves. Here, the reflection coefficient r_0 in (9) changes its sign at the Brewster angle, and according to (7) or (10) r_0 determines the sign of the reflection response of the layer. The Brewster angle is

$$\varphi_B = \arcsin\left(\frac{\rho_1^2\beta_1^4 - \rho_2^2\beta_1^2\beta_2^2}{\rho_1^2\beta_1^4 - \rho_2^2\beta_2^4}\right)^{\frac{1}{2}} \quad (=63° \text{ in our example}).$$

In cases of practical interest, φ' is normally less than φ_B. If then φ increases and exceeds φ_B, $\bar{r}(t)$ will eventually drop to zero and change its sign. This trend is evident in Fig. 5 at the largest distances. Therefore, as a rule, φ should not exceed φ_B. No such basic limitation exists for acoustic P waves, since here r_0 has the same (negative) sign for all angles of incidence.

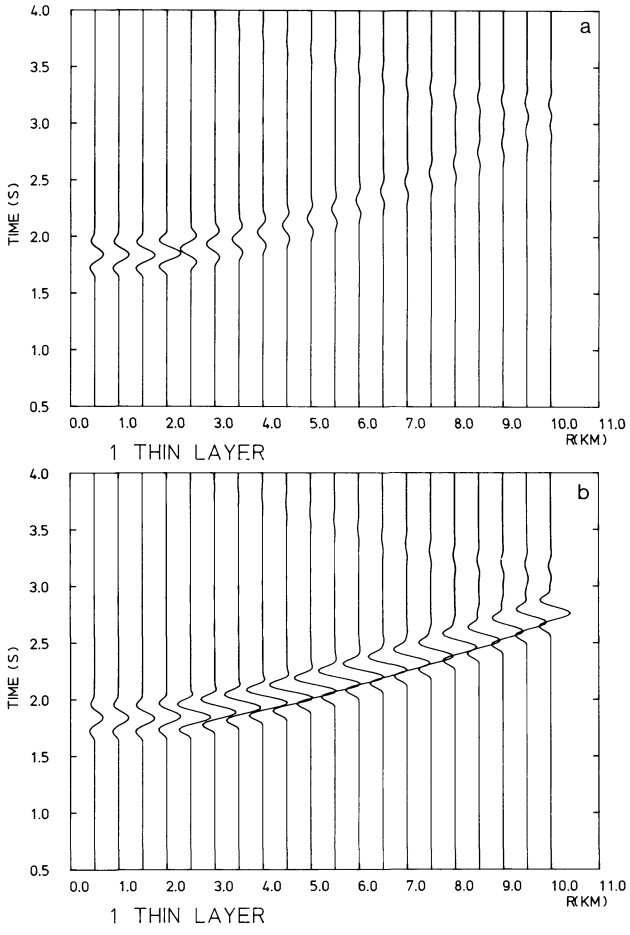

Fig. 7. a Acoustic diffraction response (vertical component) for the one-layer model of Fig. 6a. **b** The same as (**a**), but with the reflection response included

Applications

The first (purely synthetic) example is the diffraction and reflection response of a horizontal layer of finite width, excited by acoustic P waves from an explosive line source. The dimensions of the model, its parameters and the source and receiver geometry are given in Fig. 6a, and the seismograms for the vertical component in Fig. 7. The source pulse is one sine oscillation with smooth beginning and end. The dominant frequency is 2.5 Hz, corresponding to a ratio of wavelength (in the layer) to layer thickness of 240, i.e., the reflection from the layer is very well described by $r(t)$ in (10). Fig. 7a shows the two diffractions from the edges of the layer alone. The diffraction from the left edge is clearly visible, and, as expected, it changes its sign at the shadow boundary in reflection which is located at a horizontal distance of 2.0 km. The diffraction from the

right edge is rather weak, and its shadow boundary is beyond the profile section shown. Superposition of the reflection from the layer at distances greater than 2.0 km (Fig. 7b) makes the diffracted-reflected arrival continuous at the shadow boundary.

The model of the second example consists of 20 coal seams, each 1 m thick, which are offset by a fault (Fig. 6b). Such a model has been investigated by Dresen and Ullrich (1978) and Kerner (1978) with methods of model seismology. The dominant frequency is about 66 Hz, and the ratio of dominant wavelength to seam thickness is 43. The theoretical seismograms (Fig. 8) were again calculat-

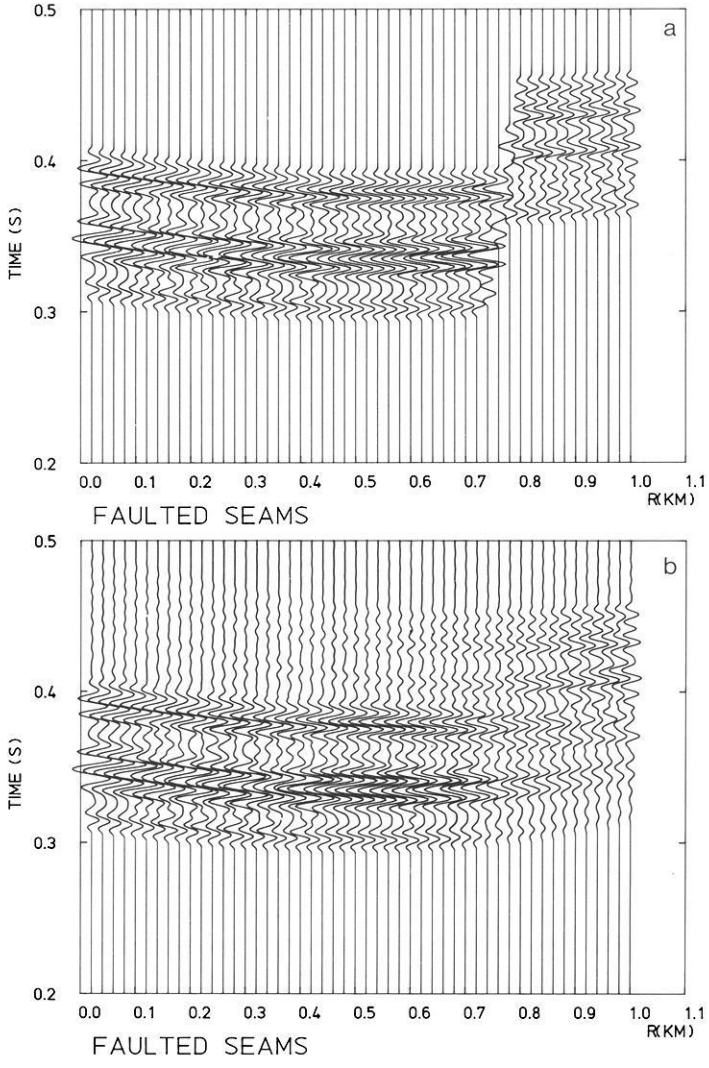

Fig. 8. a Acoustic reflection response (vertical component) for the model of faulted seams shown in Fig. 6b. **b** The same as (**a**), but with the diffractions from the seam ends at the fault included

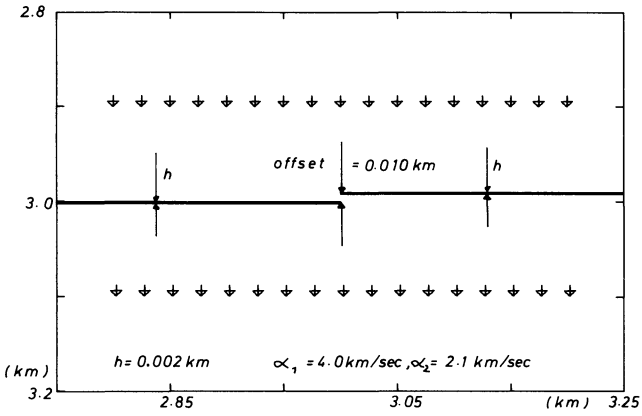

Fig. 9. Coal-seam model with an offset and two receiver profiles. For the upper profile the reflection and diffraction response is calculated (Figs. 10 and 12a), and for the lower profile the transmission and diffraction response (Figs. 11 and 12b). The density ratio is $\rho_2/\rho_1 = 0.5$. The line source is located 3 km above the offset, i.e., the incident wave is effectively plane

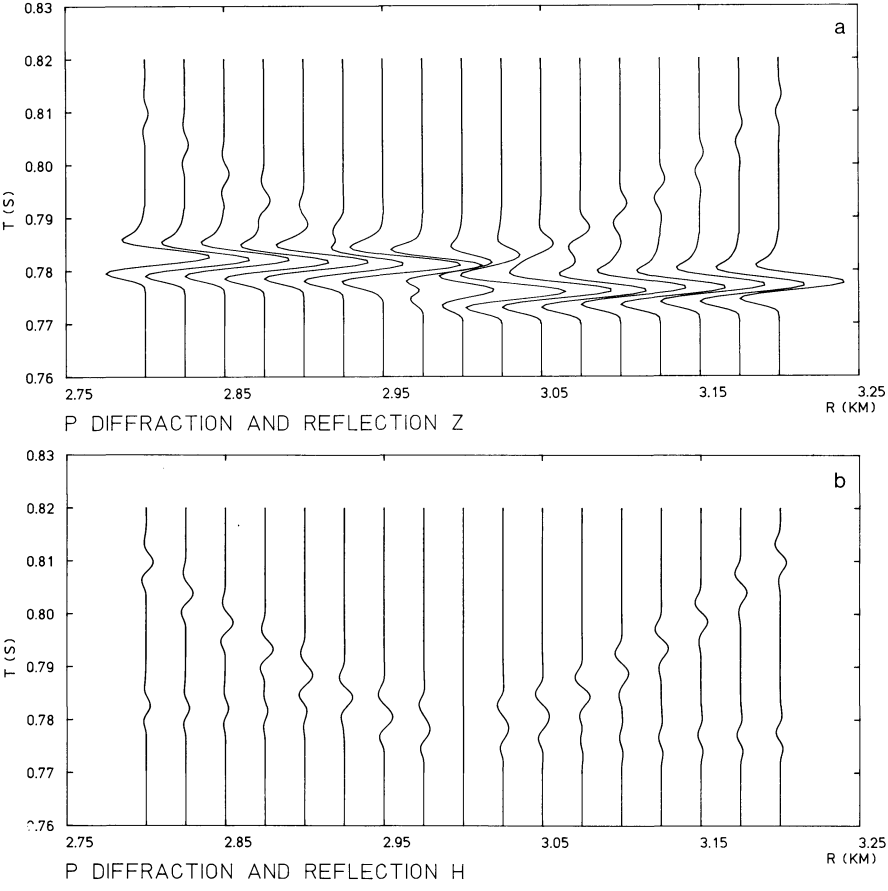

Fig. 10a and b. Acoustic reflection and diffraction response of the model in Fig. 9: **a** vertical component, **b** horizontal component. The amplitude scales in both sections are the same

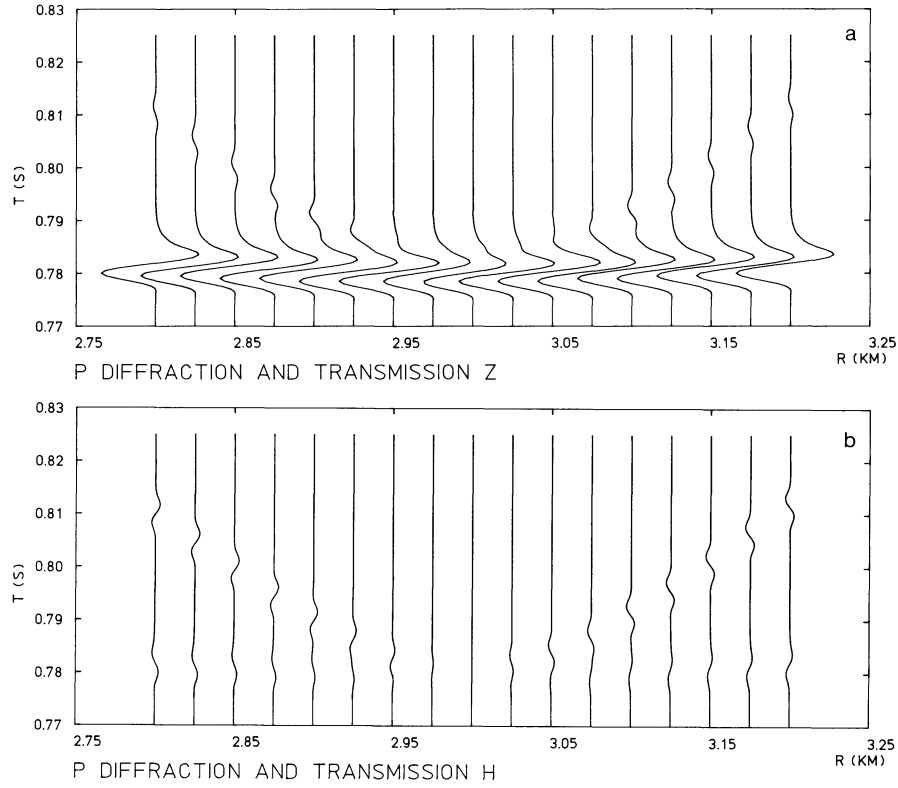

Fig. 11a and b. Acoustic transmission and diffraction response of the model in Fig. 9: **a** vertical component, **b** horizontal component. The amplitude scales in both sections are the same

ed for the acoustic case and the vertical component. Only primary reflections from the seams and primary diffractions from the seam ends were taken into account, and transmission effects at the seams were neglected. These approximations are justified for many cases of practical interest. In Fig. 8a the reflections are shown alone. They form a complicated interference pattern, consisting mainly of three wavegroups. The fault is very clear in this seismogram section. Including the diffractions from the seam ends at the fault masks the fault considerably (Fig. 8b), mainly because the reflections from the right block of seams are now weakened by the corresponding diffractions and do not stand out clearly against the diffractions from the left block which arrive earlier.

The last example deals with a realistic offset of a coal seam and the corresponding diffraction effects in the forward and backward direction for a source above the offset (Fig. 9). The situation would roughly correspond to an excitation of waves at the earth's surface and observations in tunnels close to the seam. Both the acoustic P wave case and the SH wave case have been treated for a source signal with a dominant frequency of 100 Hz (Figs. 10–12). As expected, the seam offset is most clearly seen in the reflected wave where it produces a time offset; this offset is larger for SH than for P waves because the *S*

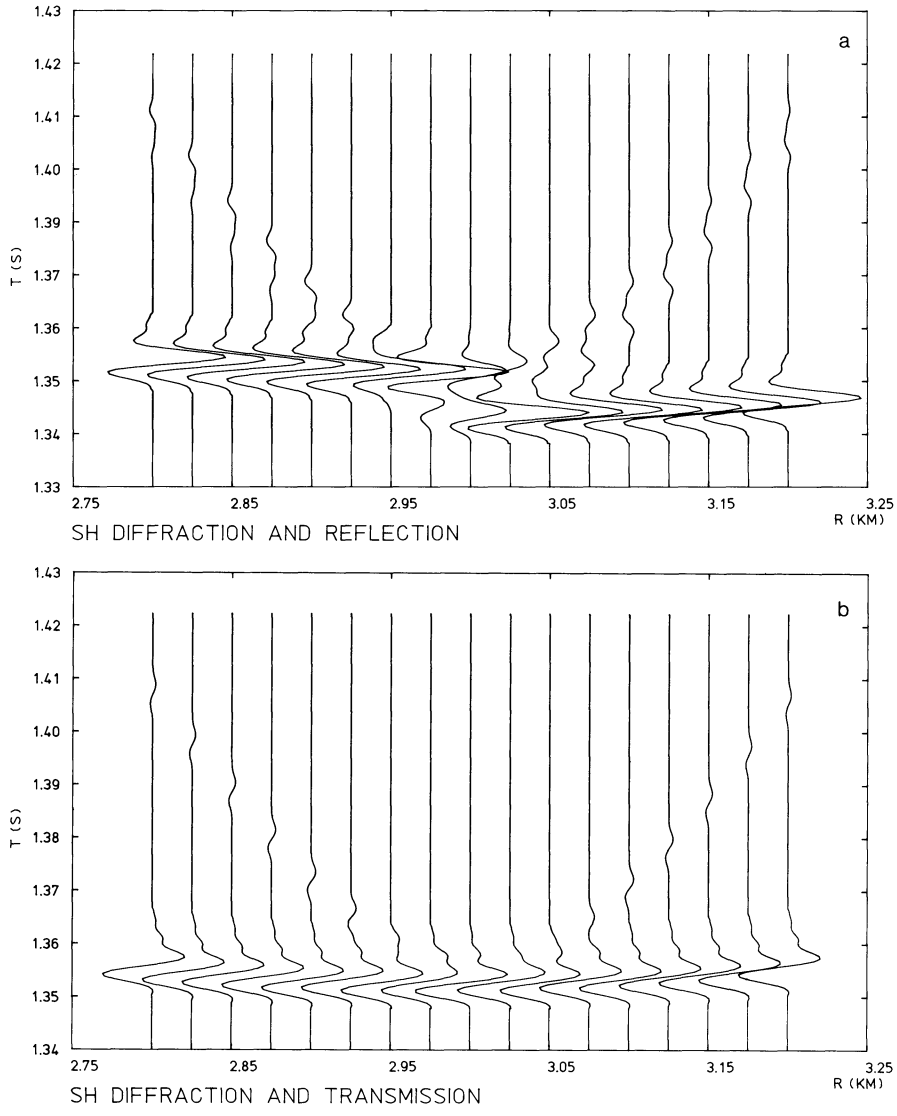

Fig. 12a and b. SH-wave reflection and diffraction response (**a**) and transmission and diffraction response (**b**) of the model in Fig. 9. The amplitude scales in both sections are the same

velocity is lower than the *P* velocity. Since in practice time offsets can also be generated by velocity heterogeneities along the whole wavepath and since they are not always eliminated by static corrections, it is reasonable to explore whether diffractions can be used, alone or additionally, to localize seam offsets. The seismograms for the horizontal component in the acoustic case (Figs. 10b and 11b) show that, indeed, diffractions may be prominent arrivals. Their prominence over the reflection or transmission in our example is due to the

large distance of the source above the seam which gives predominantly vertical polarization of the reflection and transmission. Such conditions would probably also have to exist in practical cases, but then horizontal-component recordings of P waves could actually help in identifying seam offsets. Seam depths less than the 3 km assumed in our example would require receiver profiles, which are correspondingly shorter and closer to the seam than in Fig. 9, and frequencies in excess of 100 Hz.

The applications of our computational method for theoretical seismograms show that it allows the modelling of subsurface structures typical for coal deposits; models more complicated than the one in Fig. 6b can easily be treated. Extensions of our method which have not yet been accomplished are the P–SV case and the inclusion of a layered overburden on top of the medium with the seams.

Conclusions

The reason for the relatively broad range of diffraction angles for which formula (6) is a good approximation is that the reciprocity principle has been incorporated, but it was shown that for large diffraction angles (6) is no longer applicable to SH waves. Similar restrictions could exist for other wave types, although not related to the Brewster angle. To find out where formula (6) really breaks down is a matter of further investigations and requires eventually finite-difference calculations also for the acoustic and the P–SV case.

The method for computation of theoretical seismograms presented in this paper, including both diffractions and reflected waves, allows fast calculations of the elastic response of relatively complicated structures. Therefore, it is possible to simulate effectively with this method the shooting and recording techniques of seismic prospecting such as the common-depth-point technique. The resulting seismogram sections could then be subjected to inversion procedures such as migration, and the latter would not just be the inverse operation of the modelling method. Thus, migration and other procedures could seriously be tested.

The generalization of the approximate diffraction theory for transparent half-planes to P–SV waves in solid media is straight-forward. The simplest cases are those of incident P waves and P diffractions and of incident SV waves and SV diffractions. Formula (6) can directly be applied, and the averaged plane-wave reflection and transmission responses, $\bar{r}(t)$ and $b(t)$, are those for the P–P and the SV–SV case, respectively. In the case of SV diffractions due to incident P waves (and similarly of P diffractions due to incident SV waves) the diffraction operators have to be included in the averaging process, and the geometrical spreading factors are slightly more complicated than the term $(R' + R)^{-\frac{1}{2}}$ in (6). The term of the averaging formula, which takes account of the P diffraction upon incidence of an SV wave, has to be set equal to zero for angles of incidence at the edge of the half-plane greater than the critical angle arc sin (β_1/α_1), since then no plane-wave reflection and transmission response exists.

Acknowledgments. This work was supported financially by Ruhrkohle AG and the government of Nordrhein-Westfalen. The computations were performed at the computing center, University of Karlsruhe. We thank Vlastislav Červený, Karl Fuchs, Michael Korn and Horst Stöckl for discussions on the subject of this paper, Karl Fuchs for reading the manuscript, and Ingrid Hörnchen for typing it. Contribution No. 181, Geophysical Institute, University of Karlsruhe.

References

Berryhill, J.R.: Diffraction response for nonzero separation of source and receiver. Geophysics **42**, 1158–1176, 1977

Boore, D.: Finite-difference methods for seismic wave propagation in heterogeneous materials. Methods in Computational Physics, Vol. 11. New York: Academic Press 1972

Dresen, L., Ullrich, G.: On the reflectivity of cyclically layered coal deposits – studies by means of two-dimensional models. Paper presented at 48th Annual Meeting of Society of Exploration Geophysicists, San Francisco 1978

Fertig, J., Müller, G.: Computations of synthetic seismograms for coal seams with the reflectivity method. Geophys. Prospect. **26**, 868–883, 1978

Kelly, K.R., Ward, R.W., Treitel, S., Alfred, R.M.: Synthetic seismograms: a finite-difference approach. Geophysics **41**, 2–27, 1976

Kerner, C.: Datenbearbeitung von Reflexionsseismogrammen, gemessen an Modellen des zyklisch geschichteten Steinkohlengebirges. Diploma Thesis, University of Bochum 1978

Pao, Y.-H., Mow, C.-C.: Diffraction of elastic waves and dynamic stress concentrations. 694 pp. New York: Crane Russak and London: Adam Hilger 1973

Trorey, A.W.: Diffractions for arbitrary source-receiver locations. Geophysics **42**, 1177–1182, 1977

Received August 28, 1979; Revised Version October 8, 1979